www.cambridge.org

Article-type

Keywords:

Sediment transport, remote sensing, machine learning, coastal monitoring, coastal waters

*Author for correspondence. Email: igoea@tcd.ie

Modelling suspended sediment concentration in coastal Ireland using machine learning

Aoife Igoe,* Iris Moeller, and Biswajit Basu

Trinity College Dublin, Dublin, Ireland

Abstract

Coastal environments are highly dynamic, making the monitoring of suspended sediment concentration (SSC) both challenging and essential. SSC serves as a critical indicator of coastal processes, storm impacts, water quality, and ecosystem service delivery. However, direct measurement of SSC is often prohibitively expensive, logistically difficult, and spatially limited, hindering routine monitoring by public agencies. While remote sensing offers a promising alternative by estimating SSC from surface reflectance, it typically requires extensive calibration and is often constrained by site-specific applicability.

This study presents a machine learning based framework for national-scale SSC estimation using Landsat-8 and Sentinel-2 satellite imagery, calibrated with 147 in situ SSC samples collected within one day of satellite overpass. We evaluate several models, including Random Forest, XGBoost, and deep learning approaches, with XGBoost yielding the best performance ($R^2 = 0.72$, RMSE = 17 mg/L, Bias = -1.8%). Model interpretability was supported using SHAP values (SHapley Additive exPlanations), which identified visible and infrared spectral bands, along with geographic features, especially longitude, as key predictors. This reflects the importance of coastal typology in shaping the SSC–reflectance relationship.

The model's practical value is demonstrated through a spatio-temporal analysis of SSC in Wexford Harbour using the modelled SSC from 10 years of satellite data. Seasonal patterns showed higher estuarine mixing during winter months compared to summer. High SSC events were associated with elevated daily rainfall and strong winds, indicating responsiveness to meteorological drivers at a local level.

These findings highlight the potential of integrating remote sensing and machine learning for scalable, interpretable, and cost-effective SSC monitoring, supporting data-driven research in dynamic coastal environments.

Impact Statement

Climate change and land use change are threatening the functioning and quality of coastal environments in Ireland as elsewhere across the globe. Suspended sediment concentration in coastal waters acts as an indicator of coastal dynamics, storm impact, water quality, and ecosystem service delivery. Its measurement is thus of extreme importance to coastal management and land-use planning, and capturing temporal and spatial fluctuations in suspended sediment concentrations is critical for informed environmental management and decision-making. Measuring SSC is also notoriously difficult as direct sampling of coastal waters is at best costly and at worst impossible, compromising the ability of governments and public agencies to monitor SSC. Remote sensing from aircraft or satellites allows us to estimate SSC remotely but this has other challenges, such as cloud cover or the complex way in which many constituents of coastal water (e.g. algae) reflect sunlight and complicate the SSC 'signal'. We offer a methodology for estimating SSC in the coastal waters of Ireland using machine learning. As there are some direct measurements within Irish coastal areas (from water samples largely collected to meet Ireland's obligations as part of the EU's Water Framework Directive's), we were able to compare measured with remotely estimated SSC using a combination of NASA's Landsat-8 and Copernicus Sentinel-2 satellite imagery. As the relationship between actual and satellite estimated SSC is heavily affected by the type of coast, we see an influence of geographic location on the model developed. The resultant machine learning tool has the advantage that it can be continuously improved as more satellite imagery is acquired, with minimal field sampling effort. If adopted by governments and public agencies as a tool to monitor SSC, spatially explicit coastal management and planning will improve markedly.



This peer-reviewed article has been accepted for publication but not yet copyedited or typeset, and so may be subject to change during the production process. The article is considered published and may be cited using its DOI. 10.1017/cft.2025.10016

This is an Open Access article, distributed under the terms of the Creative Commons Attribution-NonCommercial-NoDerivatives licence (http://creativecommons.org/licenses/by-nc-nd/4.0/), which permits non-commercial re-use, distribution, and reproduction in any medium, provided the original work is unaltered and is properly cited. The written permission of Cambridge University Press must be obtained for

Introduction

27

34

38

42

51

53

55

57

Suspended sediment concentration is an important parameter 80 to monitor at the coast. Changes in SSC can reflect coastal 81 erosion and affect the formation of coastal landforms, as well 82 as impacting how coastal landforms persist and continue to 83 provide coastal flood protection. Coastal wetland areas are 84 particularly sensitive to changes in SSC. Within shallow es-85 tuarine settings allochthonous (externally-derived and tidally 86 imported) sediment has been shown to be a critical deter-87 minant of an individual coastal wetland's ability to accrete 88 upwards (French et al. 1995). Once compaction and shallow 89 subsidence has been taken into account (see e.g. Allen (2000)), 90 such accumulation determines the wetland's elevation relative 91 to sea level rise. Under conditions of low wave energy, sus- 92 pended sediment can also deposit on tidal flats and influence 93 the time to maturity of salt marshes or mangroves, which pro-94 vide many important ecosystem services (Currin, Davis, and 95 Malhotra 2017; Lovelock 2008). Thus in addition to requiring 96 sufficient accommodation space (for example landwards migra- 97 tion), whether intertidal wetlands can persist in the face of a 98 rise in sea level is critically determined by suspended sediment 99 concentrations (see also Saintilan et al. (2022) and Kirwan 100 and Megonigal (2013)). Sediment in tidal waters also plays 101 an important role in impacting water quality and primary 102 production, both of which are key controls on the shallow

water marine food web (Bilotta and Brazier 2008). Spatial 104 patterns and temporal changes in SSC are thus important in 105 affecting recreational and commercial marine fisheries.

Importantly, recent global climatic and regional and local 107 land use changes have led to changes in many of the controls 108 on sediment delivery and distribution in shallow coastal seas. While land use changes such as dam construction, river dredg-110 ing and flood defences have significantly altered the release of 111 sediment from river catchments (Syvitski et al. 2005; Heritage 112 and Entwistle 2020), there has also been an increasing intensity of meteorologically induced storm surges (Debernard, 1114 Sætra, and Røed 2002; Michaels, Knappenberger, and Davis 1115 2005), and changes in the behaviour of sediment (e.g. the $_{116}$ flocculation of clay particles which is dependent on salinity $_{117}$ and flow velocities (Mietta et al. 2009)) in the coastal ocean. 118 The spatial distribution of SSC is thus of particular interest 119 in areas that have coastlines vulnerable to flooding or erosion 120 and dependent on the deposition and configuration of the shal-121 low intertidal zone. In Ireland, such areas include Wexford Harbour. In such locations, better monitoring of SSC can aid 123 in planning of adjacent land use and coastal flood risk man- $_{^{124}}$ agement. Current modelling of SSC, however, is often based on point measurements at specific locations for water quality $_{\scriptscriptstyle{126}}$ assessment, at long and irregular time-intervals. Knowledge on the spatio-temporal patterns of SSC is thus limited by the $_{\scriptscriptstyle{128}}$ spatial distribution of the sampling sites, which does not allow for sufficient frequency of observations over larger ($\geq \mathrm{km}^2$) $_{_{130}}$ areas and time periods (\geq decades).

Remote sensing of SSC

Remote sensing has become a powerful tool for monitoring inland and coastal water bodies. Earth observation satellites, such as those in the Landsat, Sentinel, and MODIS missions, acquire imagery across a range of spectral bands, from visible to near-infrared and shortwave infrared, allowing for consistent, large-scale observations of surface conditions. These sensors measure top-of-atmosphere radiance, which is processed to yield surface reflectance: the proportion of incoming solar radiation reflected by the Earth's surface back toward the sensor at different wavelengths (Wang et al. 2020).

In aquatic environments, surface reflectance is influenced by the optical properties of the water column, which are, in turn, affected by various constituents, including suspended sediments, coloured dissolved organic matter (CDOM), phytoplankton (quantified via chlorophyll-a), and dissolved substances (Gholizadeh, Melesse, and Reddi 2016). Suspended sediment concentration (SSC), in particular, plays a dominant role in modulating water-leaving reflectance, primarily through the scattering and absorption of light. Because suspended particles alter the reflectance signature in specific spectral regions it is possible to relate satellite-derived surface reflectance to SSC using a range of modelling approaches.

Analytical and semi-analytical methods require detailed information about the water column, including depth, sediment characteristics (e.g., mass, rock type, and grain size), and the relative proportions of CDOM and SSC (Wang et al. 2020). Montanher and Souza Filho (2015) found that different spectral bands were needed for modelling SSC depending on whether the water was dominated by inorganic particles or a combination of inorganic and phytoplankton. The turbidity of the water also affects the best spectral bands for modelling (Gholizadeh, Melesse, and Reddi 2016). These methods necessitate comprehensive local water studies, making the resulting models highly location-specific. Empirical methods, by contrast, rely primarily on SSC samples collected near the time of satellite image capture. These samples are used to establish a statistical relationship between surface reflectance and SSC (Wang et al. 2020). Several challenges arise when using these methods. Firstly, they often remain location-specific, as the relationship between reflectance and SSC is influenced by the particular particulate matter present, as well as water depth. Secondly, these methods require a substantial number of SSC samples collected concurrently with satellite overpasses under cloud-free conditions, particularly for dynamic areas.

Research on coastal SSC modelling has primarily focused on location-specific empirical models, often achieving good results in non-turbid waters (< 100 mg/L) using multiple spectral bands. However, in turbid waters, model performance frequently deteriorates, likely due to reflectance saturation in visible bands around 100 mg/L and in non-visible bands between 500 and 1000 mg/L (Luo et al. 2018). As a result, remote sensing based solely on surface reflectance becomes less effective for detailed SSC modelling in highly turbid waters (Shahzad et al. 2018).

Given the prevalence of local-specific models, most studies

either target highly turbid waters, such as rivers, or waters ¹⁸⁸ with low turbidity (Marinho et al. 2021). One of the major ¹⁸⁹ challenges in applying remote sensing to SSC modelling is ¹⁹⁰ obtaining a sufficiently large and representative dataset of in ¹⁹¹ situ SSC samples for calibration. This is particularly critical ¹⁹² in coastal regions, which often experience high spatial and ¹⁹³ temporal variability in SSC and are vulnerable to processes on ¹⁹⁴ instantaneous time–scales, such as localised erosion, that can ¹⁹⁵ have a high but potentially short–lived impact on sediment in ¹⁹⁶ the water column. Identifying and quantifying these changes ¹⁹⁷ is essential for effective management and mitigation strategies. ¹⁹⁸

Machine Learning models

134

135

136

138

140

142

145

148

149

150

151

152

153

154

156

157

158

160

161

162

163

164

165

167

169

171

174

176

177

178

180

182

Traditional approaches for SSC modelling in the literature often rely on regression models using one or more spectral bands (Knaeps et al. 2015). These models have used various regression forms, including linear, log-linear, and polynomial 203 equations, to relate surface reflectance to SSC. While relatively 204 simple and interpretable, such models are typically limited in 205 their ability to capture complex, non-linear relationships and 206 often require location-specific calibration. To address these 207 limitations, more recent studies have explored machine learn-208 ing (ML) techniques, including Random Forests and gradient 209 boosting methods, which offer enhanced predictive capabil-210 ities. For instance, Hu et al. (2023) combined spectral bands 211 with weather and river flow data to estimate monthly SSC 212 using a gradient boosting model in the lower Yellow River in $^{\tiny 213}$ China. Machine learning models have become increasingly 214 popular in the study of coastal sediment transport (Goldstein, Coco, and Plant 2019), driven by the growing availability of 215 remote sensing and environmental data.

However, ML models also present significant challenges.²¹⁷ Chief among these is their reliance on large, high-quality ²¹⁸ training datasets. Without sufficient data, especially labelled ²¹⁹ SSC samples, models are prone to overfitting and poor gener-²²⁰ alisation (Goldstein, Coco, and Plant 2019; Brigato and Iocchi ²²¹ 2021). This leads to overconfidence in the model and low per-²²² formance outside of the training dataset. Deep learning models, ²²³ such as neural networks, are particularly data-intensive and have seen limited application due to the high cost and logistical ²²⁴ complexity of acquiring adequate in situ samples.

Interpretability remains a key concern when applying ML ²²⁶ in environmental sciences. SHAP (SHapley Additive exPlana-²²⁷ tions) has emerged as a widely used method for interpreting ²²⁸ complex models. Rooted in game theory (Shapley et al. 1953), ²²⁹ SHAP treats each feature as a player in a cooperative game and ²³⁰ allocates the model's output to features based on their marginal ²³¹ contributions. It provides local explanations that show how ²³² individual input features influence model predictions. SHAP ²³³ is especially effective for explaining ensemble models like Ran-²³⁴ dom Forests and XGBoost, which otherwise would be a black ²³⁵ box, by looking at the importance of the features across the ²³⁶ ensemble, making it more stable for ensemble methods than ²³⁷ sensitivity analysis. It has been successfully applied in environ-²³⁸ mental modelling for feature selection, model transparency, ²³⁹ and diagnostics (Tang et al. 2022; Lundberg and Lee ²⁰¹⁷). ²⁴⁰

The primary goal of this study was to develop a model capable of capturing spatio-temporal patterns of SSC to gain insights into the dynamic nature of SSC in coastal waters, taking advantage of the spatio-temporal coverage of satellite-based remotes sensing. Information on such patterns and their dynamics over time is needed both for furthering our marine and coastal ecological and geomorphological knowledge base but also for tailoring land and coastal management practices in a way that allows adaptation to climatic change and mitigation of climate change impacts. The advantages of the model's ability to accurately detect patterns and changes in SSC, its sensitivity to variations, thus outweighs the fact that its ability to exactly predict SSC at any given point in place and time is necessarily limited.

Materials and methods

Data

Satellite Imagery

This study used imagery from the Harmonized Landsat and Sentinel-2 (HLS) dataset, developed by NASA to provide consistent surface reflectance products from Landsat-8/9 (OLI) and Sentinel-2A/B (MSI) satellites (Claverie et al. 2018). By harmonising bandpass differences, spatial resolution (30m), and applying bidirectional reflectance distribution function normalisation, the dataset enables high temporal resolution (2–3 days) through combined satellite observations. The satellite images were obtained and processed using Google Earth Engine (Gorelick et al. 2017).

Suspended Sediment Concentration data

In-situ SSC samples were obtained from the EPA and EdenIreland, covering the period 1992 to 2024, collected as part of the Water Framework Directives monitoring of Transitional and Coastal Waters (Environmental Protection Agency 2024). Only surface and grab samples were included, because the spectral signal weakens with depth (Curran and Novo 1988). Each sample was taken at a Monitoring Station, which had a unique set of co-ordinates.

Combined dataset

In order to use remote sensing imagery as input to a suspended sediment concentration model, calibration to the study area is needed. This requires a set of samples matched with satellite images within a short time period, or overpass. The number of days between sample measurement and satellite image capture, and the timing of the sample is particularly important in coastal areas where there is a high amount of change on a short scale, where the time scale and degree of such change is itself time-dependent (e.g. seasonally variable). It is thus to be expected that the accuracy of any model is improved where samples are collected as close as possible in time to the time of satellite overpass. Unfortunately, this is particularly tricky in areas that receive a lot of clouds and precipitation, such as coastal regions of Ireland, and can limit the amount of available data. This study uses a strict overpass of ≤ 1 day, which allows for a suitable range of SSC to be used for calibration, with

272

273

274

275

276

277

279

281

284

286

287

288

289

291

293

294

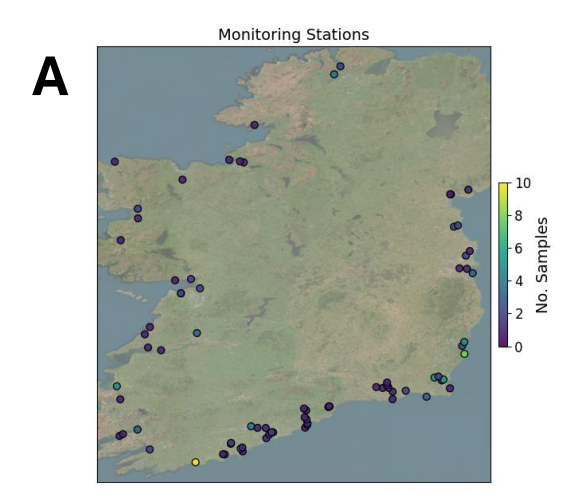
295

296

298

302

151 samples available in total. Similar studies such as Yepez 259 et al. (2018), which modelled SSC in the range of 18–203 260 mg/L used an overpass of 1 day, while Dethier, Renshaw, and 261 Magilligan (2020) tested an overpass of between 0 and 8 days 262 and found that 2 days best balanced accuracy with uncertainty 263 for their study area. The location of each monitoring station, 264 with the number of samples available is shown in Figure 1A, 265 and histogram of the suspended sediment concentration in the 266 log scale is shown in Figure 1B. There were 147 in-situ sam-267 ples that were matched with satellite images, from 78 unique 268 monitoring stations, from July 2013 to October 2024. 97 of 269 the images were from Landsat-8, and 50 were from Sentinel-2.270



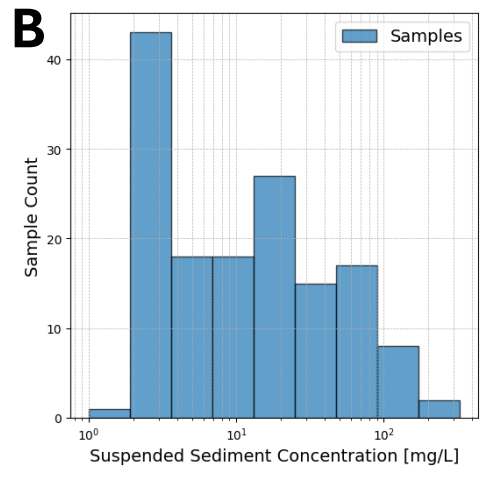


Figure 1. Location and distribution of the sampled SSC. The locations of the monitoring stations, and the number of samples from each station is shown in A, with the distribution (in the log scale) shown in B.

Methods

253

254

256

242

243

244

246

248

250

252

This study involved data pre-processing, data aggregation, and comparing modelling methods for prediction and validation of SSC. The code used to produce the results in the paper is publicly available to download on the authors GitHub repository: https://github.com/igoea20/Remote_Sensing_SSC_Ireland.

Data pre-processing

Remotely sensed spectral data requires a high-amount of preprocessing to ensure its accuracy, particularly in areas where there is a high amount of cloud cover, such as the Irish coast. Cloud and shadow masking was performed using the Fmask quality bands, masking cirrus, cloud, cloud shadow, and cloudadjacent pixels based on the approach described by Qiu, Zhu, and He (2019). Known limitations of the S30 cloud detection are addressed using a time series outlier filtering method adapted from Chen and Guestrin (2016), which applies a Hampel filter and temporal consistency analysis using the modified Normalised Difference Water Index (mNDWI), which is a ratio of the green (0.53 – 0.59 μm) and Shortwave Infrared (1.57 - 1.65 μm) bands (Claverie et al. 2018; Vermote, Justice, and Bréon 2008). Cloud-contaminated or physically implausible values (e.g., negative reflectance) were removed. Water pixels were identified using the mNDWI (Xu 2006).

For the in situ samples of SSC, some data points had to be removed due to their unsuitability to remote sensing. Measurements from water shallower than 1m were excluded to reduce errors from sediment bed backscattering. Only samples from depths \leq 5m were used to ensure that the satellite-derived signal corresponded to the upper water column, as the penetration reduces with turbidity (Curran and Novo 1988).

Random Forest

Random Forest regression, an ensemble method based on decision trees, was implemented using Scikit-learn (Pedregosa et al. 2011). It uses bootstrap samples to train individual trees, with predictions averaged to improve accuracy and reduce overfitting. To use RF models it is necessary to adjust the model's hyperparameters to suit the data and problem in question. RandomizedSearchCV was used to randomly search a grid of hyperparameters, choosing the optimal hyperparameters that minimised RMSE. The optimal hyperparameters found were: number estimators of 50, min samples in a split of 2, min samples in a leaf of 1, max features of 1, and max depth of 7.

Extreme Gradient Boosting

XGBoost (Chen and Guestrin 2016), a gradient boosting framework, builds sequential models where each minimises the errors of its predecessor, with the model consisting of many weak learners (small regression models), and the final predictions being the weighted sum of the predictions from the weak learners. It has improved control against overfitting compared to Random Forest through regularisation. The XGBoost library (version 2.1.2) was used (Chen et al. 2016), with hyperparameters tuned using RandomizedSearchCV. The optimal hyperparameters found were: number of trees of 100, tree depth of 4, learning rate of 0.03, subsample of 0.7. To improve the model interpretability, SHapley Additive exPlanations (SHAP) values were computed for the final XGBoost model, allowing insight into feature contributions and reducing its "black box" nature.

Multi-Layer-Perceptron (MLP)

312

313

314

315

316

317

318

319

320

322

323

325

327

329

331

333

334

335

336

337

338

330

340

341

342

343

MLP is a simple form of feedforward artificial neural network, ³⁵⁶ and was implemented using Scikit-learn (Pedregosa et al. 2011). Due to the limited number of samples available for training, it was configured with one hidden layer. Hyperparameters such as the number of neurons in the hidden layer, learning rate, and regularisation strength were optimised using RandomizedSearchCV. The optimal hyperparameters found were: solver = 'adam', initial learning rate = 0.03, hidden layer size = 10, alpha = 0.01, activation = 'relu'.

Input Variables

Input features to the model included the spectral bands, band ratios, and spatial coordinates. The coordinates were included 358 to account for regional environmental gradients and poten– 359 tial spatial autocorrelation. The input vector was as follows: 360 ['Blue', 'Red', 'Green', 'NIR Narrow', 'Blue/Red', 'Blue/Green', 361 'Red/Green', 'SWIR 1', 'Latitude', 'Longitude'], where Blue 362 (0.45–0.51 µm), Red (0.64 – 0.67 µm), Green (0.53–0.59 µm) 363 are the visible bands, NIR Narrow (0.85 – 0.88 µm) is the Near– 364 Infrared band, and SWIR 1(1.57 – 1.65 µm) is the Shortwave 365 Infrared band.

Model Evaluation

Model performance was evaluated using Leave One Out Cross 370 Validation (LOOCV) (Hastie et al. 2005). In this approach, the 371 dataset of size N is split into N iterations, each using $N-1_{372}$ samples for training and the remaining one for testing. This 373 method ensures each data point is tested once, providing an 374 unbiased estimate of model generalisation, and ensuring the 375 performance is reflective of the whole dataset. Model per-376 formance was evaluated using the root mean squared error 377 (RMSE, Equation 1), the coefficient of determination (R^2 , 378 Equation 2), and the relative percentage bias (Equation 3), 379 where SSC_i is the true in-situ value of SSC for observation i, \overline{SSC} is 381 the mean value of observed SSC, and n is the total number of 382 observations.

$$RMSE = \sqrt{\frac{\sum (SSC_i - S\hat{S}C_i)^2}{n}}$$
 (1)

$$R^{2} = 1 - \frac{\sum (SSC_{i} - S\hat{S}C_{i})^{2}}{\sum (SSC_{i} - \overline{SSC})}$$
 (2)

Rel. Bias =
$$100 \times \frac{\frac{1}{n} \sum (S\hat{S}C_i - SSC_i)}{\overline{SSC}}$$
 (3)

Results

353

Model Performance

The results for all three modelling approaches are shown in ³⁹⁵ Table 1. The XGBoost method demonstrated the highest ³⁹⁶ model performance with R^2 = 0.72, RMSE = 17 mg/L, Rel ³⁹⁷ Bias = -1.8%. The scatter plot in Figure 2A) shows the results ³⁹⁸ from the LOOCV predictions, compared to the in situ samples.³⁹⁹

Overall the model was able to learn the distribution, but there was a lot of scatter around the y = x line.

Table 1. Results from LOOCV of the machine learning models.

Model	RMSE [mg/L]	R^2	Rel. Bias (%)
Random Forest	19	0.65	-0.68
MLP	23	0.47	2.77
XGBoost	17	0.72	-1.8

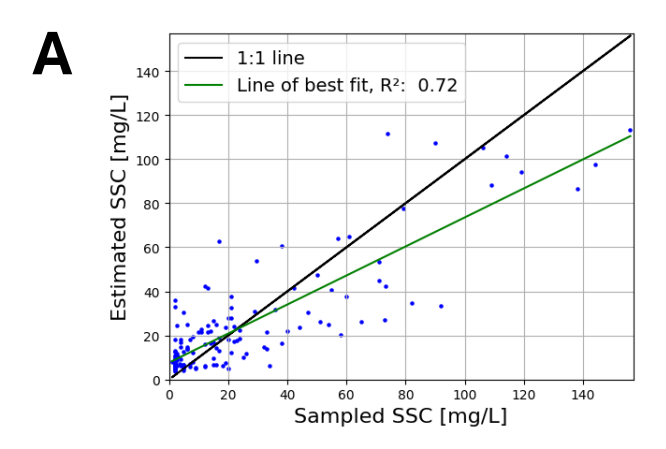
Feature Importance

Figure 2B) shows the SHAP summary plot of the XGBoost model, indicating the impact of each feature on the SSC output. The x-axis shows the SHAP value of each feature, with a value >0 indicating that the feature pushed the prediction higher, and a value <0 means the feature lowered the predicted SSC. The colour of each point indicates whether the feature value was high or low. Each point indicates a training point in the model. Longitude is shown to have the largest overall impact on model predictions, with higher values (the east of the country), tending to increase SSC. This suggests that regional differences, such as contrasting geology, sedimentology, and glacial history, as well as exposure to the predominant westerly airflow, strongly influence SSC, and we can see that there is a non-linear relationship, as expected (Devoy et al. 2021). The red and blue bands both have significant influence on SSC, with lower red or blue values tending to decrease SSC. Latitude is less important, but we can see that there is an indication of north-south differences, with higher latitude tending to decrease SSC. The other bands (non-visible NIR Narrow and SWIR 1, and band ratios) have less of an impact on SSC, and they tend to show complex relationships with SSC, due to the relationship being non-linear. We see that a high Blue/Green is associated with lower SSC (lower turbidity). A combination of short and long wavelengths takes advantage of deeper water penetration and sensitivity to high values of SSC (Curran and Novo 1988).

Several monitoring stations had consistently high prediction error (>20 mg/L), some of these locations are shown in Figure 3. The error in the monitoring stations can be explained as follows: In A there is wave breaking and diffraction around a man made structure, in B there is shallow water wave shoaling, in C it is a shallow subtidal area with surface reflectance of the bed changing between low and high tide (spring tidal range of 1.5m, neap of 0.9m (Hartnett and Nash 2004)), in D there is an artificial surface above the waterbody, in E and F there are tidal inner estuary channels.

Seasonal and event-based patterns in SSC

The developed model facilitates investigation of both seasonal variations and event-driven anomalies in SSC. Figure 4 illustrates the seasonal distribution of SSC within Wexford Harbour, comparing the winter period (December 2022 to February 2023) with the summer period (June 2023 to August 2023).



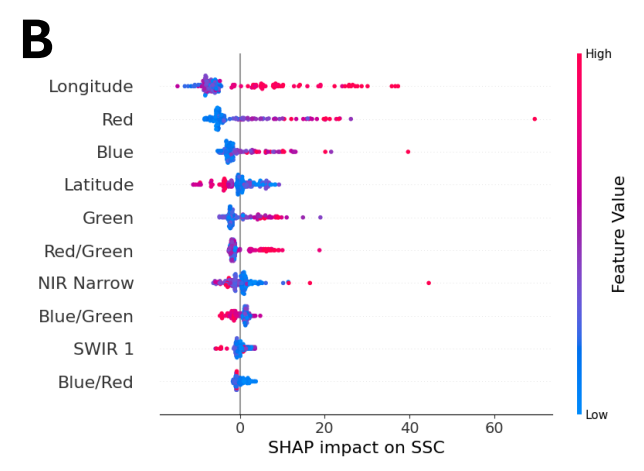


Figure 2. A) The modelled SSC, using the XGBoost model, is shown in blue. Each point is from a LOOCV iteration. The green line shows a linear regression between observed and predicted SSC. B) The SHAP analysis of the input features is shown, with the x-axis showing whether the feature increased or decreased SSC. The colorbar indicates whether the sample had a high or low value for that feature.

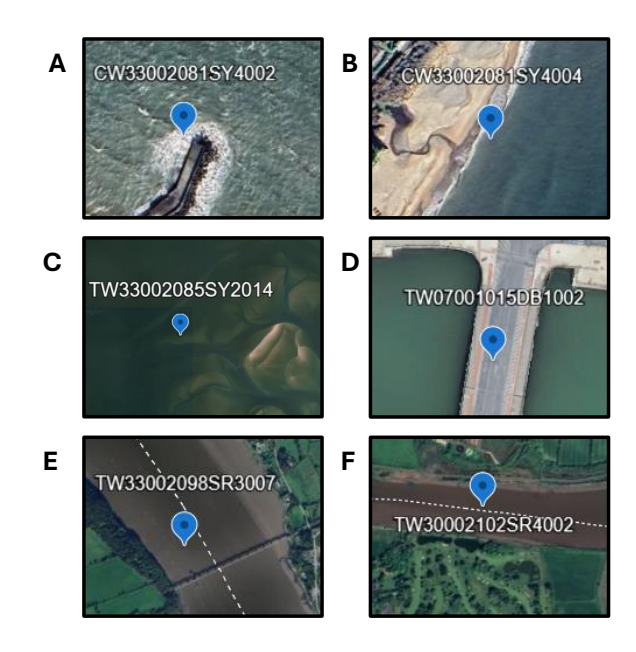


Figure 3. Six monitoring stations were identified that could not be accurately predicted using the model.

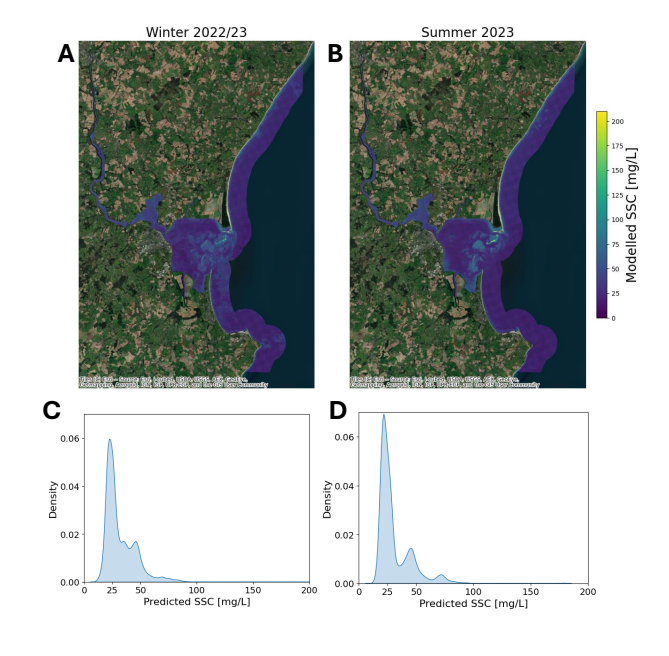


Figure 4. The seasonal median SSC is shown for Wexford Harbour. A) shows the SSC from December 2022 to February 2023. B) Shows the SSC from June 2023 to August 2023. The distribution of SSC for A) is shown in C), and the distribution of B) is shown in D).

435

436

437

438

439

441

443

444

445

447

448

449

450

452

454

456

457

458

459

460

461

462

469

470

471

Figure 5 provides additional insight into potential envi-418 ronmental drivers of extreme SSC events. Figure 5A) displays 419 the monthly distribution of daily total rainfall and average 420 windspeed measured at Johnstown Castle in Wexford over the 421 period 2014–2024. Superimposed red lines indicate years in 422 which SSC exceeded 140 mg/L, highlighting the temporal 473 alignment between extreme SSC values and weather extremes.424 Between 2014 and 2025, eight SSC measurements exceeded 425 140 mg/L, spanning five unique dates: 03/10/2019, 19/10/2022, 426 08/07/2023, 27/09/2023, and 13/06/2024. These events were 427 cross-examined against concurrent meteorological conditions. 428 Notably, the SSC peak in June 2024 coincided with anomalously high daily rainfall for that month, as seen in Figure 5B).430 Similarly, high-rainfall conditions were also observed during 431 the SSC peaks in September 2023 and October 2022, Figure 432 5C) shows that the SSC events on 27/09/2023 and 03/10/2019 433 corresponded to days with unusually high windspeed for those months.

400

401

402

403

405

406

407

409

410

411

413

414

415

416

417

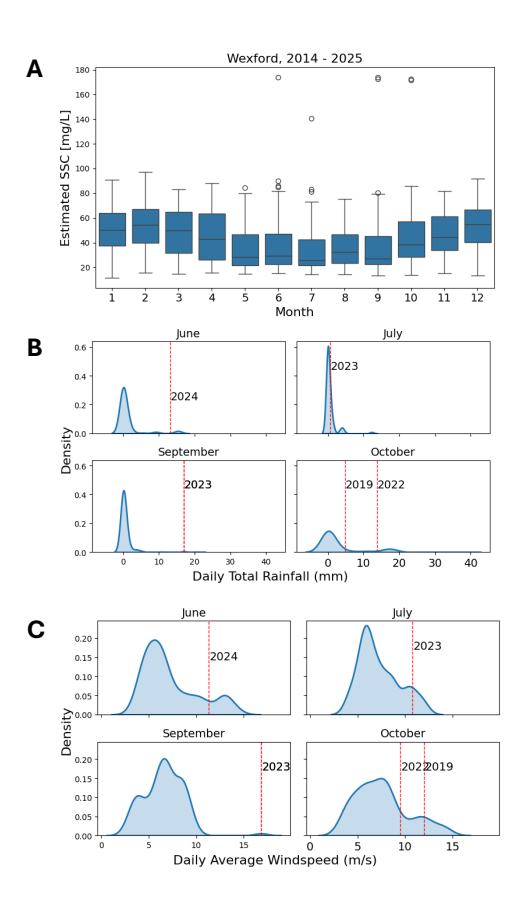


Figure 5. A) The monthly distribution of daily total rainfall measured at Johnstown Castle in Wexford. The red lines mark the years that had SSC values over 140 mg/L in that month. B) The monthly distribution of daily 466 average windspeed measured at Johnstown Castle in Wexford. The red lines 467 mark the years that had SSC values over 140 mg/L in that month.

Discussion

The XGBoost model had the highest R^2 value and lowest RMSE, and was chosen as the best of the machine learning models tested for remotely-sensed SSC in coastal Ireland. Feature attribution using SHAP (SHapley Additive exPlanations) analysis provided additional insights into the model's behavior. Among the input features, longitude was more influential than latitude, indicating a pronounced east—west spatial gradient in the SSC–spectral reflectance relationship. This spatial dependency is likely due to differences in coastal geomorphology, hydrodynamics, and sediment characteristics between the Irish Sea and Atlantic-facing coasts, and exposure to the predominant westerly airflow (Gallagher, Tiron, and Dias 2014), (Devoy 2008). SHAP analysis also confirmed that the visible bands, particularly blue, green, and red, were among the most important spectral features.

Interpreting trends in SSC

In Figure 4 a clear seasonal signal is evident, with more mixing in the winter months. Although the median SSC for the whole estuary is similar (32 mg/L for winter and 31 mg/L for summer), the spatial distribution of SSC is different as seen in Figure 4 C and D. In summer 70% of the pixels are less than 30 mg/L, compared to 60% in winter. The maximum SSC in winter is 209 mg/L in winter and 179 mg/L in summer. This pattern of elevated SSC in a wider spatial area may be attributed to increased hydrodynamic activity, including higher river discharge and wind-driven resuspension during the winter season. Bowers, Boudjelas, and Harker (1998) identified strong seasonal variations in suspended sediment in the Irish Sea.

The model also facilitates the identification and analysis of extreme suspended SSC events, as illustrated in Figure 5. When examined alongside concurrent meteorological data, including daily total rainfall and average windspeed, these high-SSC episodes frequently coincide with periods of intense weather activity. In the Wexford Harbour case study, six remote-sensing detected SSC peaks were investigated. Of these, three were associated with anomalously high monthly rainfall, while four corresponded with elevated wind speeds. These observations are consistent with previous findings suggesting that both runoff and wind-driven resuspension significantly influence episodic increases in SSC (Drewry, Newham, and Croke 2009; Kalnejais et al. 2007). Fluvial input, in particular, emerges as a likely contributor to such events, while windspeed appears to play an additional role in mobilising and resuspending sediments, further elevating SSC levels. Further research, with additional data for a greater set of extreme events could allow for a better understanding of the drivers of SSC and whether it is from runoff or wind-driven resuspension. To understand this relationship from a causal standpoint we suggest further development of methodology.

Meteorological records also indicate the occurrence of named storms in close temporal proximity to several of the identified SSC events. Notably, Storm Agnes occurred on 27 September 2023, coinciding with one of the highest SSC values observed during the study period. Similarly, Storm

540

Lorenzo impacted the region on 4 October 2019, shortly af-528 ter an SSC spike recorded on 3 October 2019 (Met Éireann 529 2025). These temporal alignments reinforce the hypothesis 530 that extreme weather events can act as significant triggers for 531 abrupt increases in coastal SSC (Miller 1999; Suursaar, Jaagus, 532 and Tõnisson 2015).

Collectively, these findings highlight the model's capabil-534 ity to capture both spatial and temporal variability in SSC. In 535 addition to identifying high-SSC zones and seasonal trends, it 536 proves effective in detecting episodic events linked to environ-537 mental drivers such as rainfall anomalies, storm activity, and 538 wind-induced resuspension.

Study limitations and next steps

474

475

477

478

479

480

481

482

483

484

487

489

490

491

492

493

495

496

497

498

500

502

504

506

508

509

511

512

513

515

516

517

518

519

520

521

522

A key limitation of the model lies in its reduced accuracy at 543 higher SSC (>75 mg/L) levels. This issue is evident in Fig-544 ure 2 and is consistent with previous findings on reflectance 545 saturation at elevated SSCs (Curran and Novo 1988; Shahzad 546 et al. 2018; Markert et al. 2018). Reflectance becomes less sensi-547 tive to additional suspended material beyond certain thresholds, 548 particularly due to the optical saturation of visible and near-549 infrared bands (Luo et al. 2018; Bowers, Boudjelas, and Harker 550 1998; Doxaran et al. 2002). Moreover, machine learning mod-551 els such as XGBoost and Random Forest are inherently non-552 extrapolative, meaning their predictions are restricted to the 553 range observed in the training data (Chen and Guestrin 2016). 554 Therefore, caution is needed when interpreting model outputs in high-turbidity regimes, and they should not be treated as absolute estimates outside the validated range. A major contribut-555 ing factor to this limitation is the under-representation of high-556 SSC samples in the training dataset. Expanding the calibration 557 dataset to better capture high-turbidity conditions would be 558 a logical next step. Targeted field sampling in known high-559 turbidity areas, coordinated with satellite overpasses, could 560 enhance the model's predictive power and ability to model 561 extreme sediment conditions.

Figure 3 highlights several monitoring stations where SSC 563 predictions were problematic. These cases emphasise the im-564 portance of quality control in calibration data and the need for 565 manual inspection and filtering to ensure representativeness.566 Remote sensing models must also be applied cautiously, par-567 ticularly in tidal areas where water depth fluctuates and may 568 push pixels in and out of the valid range for SSC estimation 569 (Dethier, Renshaw, and Magilligan 2020; Pahlevan et al. 2017).570

The lack of high-resolution, up-to-date bathymetry data 571 for Ireland's coastal waters presents an additional constraint 572 (O'Toole et al. 2022). Without accurate bathymetric infor-573 mation, the reliability of reflectance-based SSC estimates di-574 minishes in shallow or variable-depth regions. Addressing 575 this will require improved tidal prediction tools and detailed 576 bathymetric surveys to support broader operational use.

This study also raises broader questions around the com-578 plexity and interpretability of machine learning models in envi-579 ronmental science. While achieving high predictive accuracy 580 is important, it must not come at the expense of transparency 581 and rigorous validation. This includes using cross-validation, 582

multiple performance metrics, and interpretability tools such as SHAP values. However, it's important to note that SHAP, while useful, only provides correlational insight. Moreover, model performance is constrained by the quality and size of the training data, requiring thoughtful choices around regularisation, architecture, and parameter tuning—especially in deep learning models such as neural networks (Zhu, Yang, and Ren 2023; Karpatne et al. 2018).

Although results were visualised using downsampled outputs for clarity, the model retains its full 30m spatial resolution, enabling fine-scale environmental monitoring in regions as small as $5\ km^2$. This makes the method particularly well-suited for event-based studies (e.g., storms or floods), multi-year trend assessments, and local-scale management decisions. For example, it can help evaluate post-construction sediment changes around coastal infrastructure (e.g., breakwaters or tidal barrages) by comparing recent SSC patterns to historical baselines. It also holds promise for the long-term monitoring of sediment-sensitive ecosystems such as estuaries, saltmarshes, and wetlands.

In addition to expanding the dataset and improving bathymetry, future research could explore the use of causal inference methods to go beyond correlational models and gain a mechanistic understanding of the drivers of SSC variability. This could yield more actionable insights for environmental planning and policy, especially in coastal zones prone to rapid sediment changes.

Conclusions

In this study, we developed and validated a machine learning approach for modelling SSC in coastal areas using remote sensing data, incorporating geographic information to improve predictive accuracy. Our model, based on XGBoost, integrated visible and infrared spectral bands from Landsat and Sentinel satellites with spatially explicit geographic data, and was rigorously evaluated using leave-one-out cross-validation.

The model effectively captured key spatio-temporal patterns of relative SSC in shallow coastal waters, demonstrating strong performance across multiple scales. At the regional level, it successfully identified SSC dynamics across thousands of kilometres surrounding the island of Ireland. At the local scale, its application to multi-temporal imagery of Wexford, Ireland, revealed seasonal and event-driven sediment patterns that were consistent with known meteorological, hydrodynamic, and fluvial processes at that site. Wexford estuary is a drowned valley estuary with a barrier, with flood-tidal dominance. Sediment supply forming the sediment deposits is heavily impacted by seasonal tides and flooding, with a large internal fetch distance meaning that waves are generated that can resuspend SSC and modify the shoreline (Cooper 2006).

Given the complexity and variability of Ireland's coastal zones, shaped by a range of environmental drivers, our findings are encouraging. They indicate that this modelling framework can accommodate location-specific dynamics within a unified and scalable SSC monitoring approach. While further refinement is warranted, particularly through more sophisticated

678

679

680

integration of geographic information, such as geographic re-634 gression techniques or spatial clustering of regions, our results 635 highlight the potential of remote sensing-based SSC monitor-636 ing. Such methods can support local and national agencies in 637 tracking sediment dynamics across seasonal to multi-annual 638 timeframes and spatial scales ranging from tens of meters to the 640 national level. Ultimately, this approach can inform adaptive land and coastal management strategies that promote ecologi-642 cal resilience, geomorphological stability, and climate adapta-643 tion in dynamic coastal environments.

Acknowledgement

586

588

589

590

597

598

599

600

602

605

606

607

609

610

611

615

616

621

622

623

624

625

627

628

629

630

631

632

633

The authors acknowledge that raw station datasets from Met 648 Éireann are published under Creative Commons Attribution 649 4.0 International (CC BY 4.0). (https://creativecommons.org/650 licenses/by/4.0/, last access: 15 June 2025). Additionally, it 651 is acknowledged that the processed CSV station data were 652 conducted solely by the authors of this research.

Author Contribution Statement Methodology: A.I.; I.M; 656 B.B. Data preparation: A.I. Data visualisation: A.I. Writing 657 original draft: A.I; I.M. Writing review & editing: A.I.; I.M.; 658 B.B. All authors approved the final submitted draft.

Data Availability Statement The Landsat-HLS and Sentinel-661 HLS data (available online at) were accessed using Google 662 Earth Engine and are freely available.

The processed satellite datasets and trained models are avail-665 able from the corresponding author, A.I., upon reasonable request, excluding the original dataset of in-situ samples pro-667 vided by the Environmental Protection Agency.

The python scripts used for data pre-processing, model training, and result visualisation are available at https://github.669 com/igoea20/Remote_Sensing_SSC_Ireland.

Financial Support The authors are grateful for the financial ⁶⁷³ support provided by the Provost's Council, Trinity College ⁶⁷⁴ Dublin for this work under the Prendergast Challenge Based ⁶⁷⁵ Award for the project 'Life in the Currents'.

Competing Interests The authors declare none.

References

- Allen, J.R.L. 2000. Morphodynamics of holocene salt marshes: a review sketch ⁶⁸² from the atlantic and southern north sea coasts of europe. *Quaternary* ⁶⁸³ *Science Reviews* 19 (12): 1155–1231. https://doi.org/10.1016/S0277-684 3791(99)00034-7.
- Bilotta, G.S., and R.E. Brazier. 2008. Understanding the influence of suspended 686 solids on water quality and aquatic biota. *Water Research* 42 (12): 2849–687 2861. https://doi.org/10.1016/j.watres.2008.03.018.
- Bowers, DG, S Boudjelas, and GEL Harker. 1998. The distribution of fine 689 suspended sediments in the surface waters of the irish sea and its relation 690 to tidal stirring. *International Journal of Remote Sensing* 19 (14): 2789–691 2805. https://doi.org/10.1080/014311698214514.
- Brigato, Lorenzo, and Luca Iocchi. 2021. A close look at deep learning with ⁶⁹³ small data. In *2020 25th international conference on pattern recognition (icpr)*, ⁶⁹⁴ 2490–2497. IEEE. https://doi.org/10.48550/arXiv.2003.12843.

- Chen, Tianqi, et al. 2016. *Xgboost: extreme gradient boosting.* https://xgboost.readthedocs.io/. Python package version 2.1.2.
- Chen, Tianqi, and Carlos Guestrin. 2016. XGBoost: a scalable tree boosting system. In *Proceedings of the 22nd acm sigkdd international conference on knowledge discovery and data mining*, 785–794. KDD '16. San Francisco, California, USA: ACM. ISBN: 978-1-4503-4232-2. https://doi.org/10.1145/2939672.2939785. http://doi.acm.org/10.1145/2939672.2939785.
- Claverie, Martin, Junchang Ju, Jeffrey G. Masek, Jennifer L. Dungan, Eric F. Vermote, Jean-Claude Roger, Sergii V. Skakun, and Christopher Justice. 2018. The harmonized landsat and sentinel-2 surface reflectance data set. *Remote Sensing of Environment* 219:145–161. https://doi.org/10.1016/j.rse.2018.09.002.
- Cooper, JAG. 2006. Geomorphology of irish estuaries: inherited and dynamic controls. In Proceedings of the 8th international coastal symposium (ics 2004), 176–180. Journal of Coastal Research. https://www.jstor.org/stable/ 25741557.
- Curran, Paul James, and EMM Novo. 1988. The relationship between suspended sediment concentration and remotely sensed spectral radiance: a review. *Journal of Coastal Research*, 351–368. https://www.jstor.org/stable/4297423.
- Currin, Carolyn A, Jenny Davis, and Amit Malhotra. 2017. Response of salt marshes to wave energy provides guidance for successful living shoreline implementation. Chap. 11 in *Living shorelines*, 211–234. CRC Press. https://doi.org/10.1201/9781315151465-14.
- Debernard, Jens, Øyvind Sætra, and Lars Petter Røed. 2002. Future wind, wave and storm surge climate in the northern north atlantic. *Climate research* 23 (1): 39–49. https://doi.org/10.3354/cr023039.
- Dethier, E. N., C. E. Renshaw, and F. J. Magilligan. 2020. Toward improved accuracy of remote sensing approaches for quantifying suspended sediment: implications for suspended-sediment monitoring. *Journal of Geophysical Research: Earth Surface* 125 (7): e2019JF005033. https://doi.org/10.1029/2019JF005033.
- Devoy, Robert, Andrew J. Wheeler, Barry Brunt, and Kieran Hickey. 2021. The coastal environment: physical systems, processes and patterns. Chap. 2 in *The coastal atlas of ireland*. Cork University Press.
- Devoy, Robert JN. 2008. Coastal vulnerability and the implications of sealevel rise for ireland. *Journal of Coastal Research* 24 (2): 325–341. https://doi.org/10.2112/07A-0007.1.
- Doxaran, David, Jean-Marie Froidefond, Samantha Lavender, and Patrice Castaing. 2002. Spectral signature of highly turbid waters: application with spot data to quantify suspended particulate matter concentrations. *Remote sensing of Environment* 81 (1): 149–161. https://doi.org/10.1016/S0034-4257(01)00341-8.
- Drewry, JJ, LTH Newham, and BFW Croke. 2009. Suspended sediment, nitrogen and phosphorus concentrations and exports during storm-events to the tuross estuary, australia. *Journal of environmental management* 90 (2): 879–887. https://doi.org/10.1016/j.jenvman.2008.02.004.
- Environmental Protection Agency, EPA. 2024. Unpublished dataset. Data provided by [Environmental Protection Agency, Castlebar, Ireland]. Provided on [15/05/2024].
- French, JR, T Spencer, AL Murray, and NS Arnold. 1995. Geostatistical analysis of sediment deposition in two small tidal wetlands, norfolk, uk. *Journal of Coastal Research*, no. 2, 308–321. http://www.jstor.org/stable/4298342.
- Gallagher, Sarah, Roxana Tiron, and Frédéric Dias. 2014. A long-term nearshore wave hindcast for ireland: atlantic and irish sea coasts (1979–2012) present wave climate and energy resource assessment. Ocean Dynamics 64 (August): 1163–1180. https://doi.org/10.1007/s10236-014-0728-3.
- Gholizadeh, Mohammad Haji, Assefa M. Melesse, and Lakshmi Reddi. 2016. A comprehensive review on water quality parameters estimation using remote sensing techniques. Sensors 16 (8). https://doi.org/10.3390/ s16081298.

807

808

809

810

811

Goldstein, Evan B, Giovanni Coco, and Nathaniel G Plant. 2019. A review of 751 machine learning applications to coastal sediment transport and mor-752 phodynamics. Earth-science reviews 194:97-108. https://doi.org/10.1016/753 j.earscirev.2019.04.022. 699

697 698

700

701

702

703

705

706

714

715

716

717

719

720

721

722

723

724

725

726

730

731

732

733

734

735

736 737

742

743

744

745

- Gorelick, Noel, Matt Hancher, Mike Dixon, Simon Ilyushchenko, David Thau, and Rebecca Moore. 2017. Google earth engine: planetary-scale 757 geospatial analysis for everyone. Remote Sensing of Environment 202:18-758 27. https://doi.org/10.1016/j.rse.2017.06.031.
- Hartnett, Michael, and Stephen Nash. 2004. Modelling nutrient and chloro-759 phyll_a dynamics in an irish brackish waterbody. *Environmental Mod*⁷⁶⁰ elling & Software 19 (1): 47-56. https://doi.org/10.13025/18597. 761
- Hastie, Trevor, Robert Tibshirani, Jerome Friedman, and James Franklin. 762 707 2005. The elements of statistical learning: data mining, inference and 763 708 prediction. The Mathematical Intelligencer 27 (2): 83–85. https://doi.org/ 709 10.1007/BF02985802. 710
- Heritage, George, and Neil Entwistle. 2020. Impacts of river engineering on 711 river channel behaviour: implications for managing downstream flood 767 712 risk. Water 12 (5): 1355. https://doi.org/10.3390/w12051355. 713
 - Hu, Jinlong, Chiyuan Miao, Xiangping Zhang, and Dongxian Kong. 2023. Retrieval of suspended sediment concentrations using remote sensing and machine learning methods: a case study of the lower yellow river. Journal of Hydrology 627:130369. https://doi.org/10.1016/j.jhydrol.2023.772 130369 773
 - Kalnejais, Linda H, William R Martin, Richard P Signell, and Michael H 774 Bothner. 2007. Role of sediment resuspension in the remobilization of 775 particulate-phase metals from coastal sediments. Environmental Science & 776 Technology 41 (7): 2282–2288. https://doi.org/10.1021/es061770z.
 - Karpatne, Anuj, Imme Ebert-Uphoff, Sai Ravela, Hassan Ali Babaie, and Vipin Kumar. 2018. Machine learning for the geosciences: challenges and 779 opportunities. IEEE Transactions on Knowledge and Data Engineering 31 (8): 1544–1554. https://doi.org/10.1109/TKDE.2018.2861006.
- 727 Kirwan, Matthew L, and J Patrick Megonigal. 2013. Tidal wetland stability in the face of human impacts and sea-level rise. *Nature* 504 (7478): 53–60. 728 729 https://doi.org/10.1038/nature12856.
 - Knaeps, Els, Kevin G Ruddick, David Doxaran, Anna I Dogliotti, Bouchura 786 Nechad, D Raymaekers, and S Sterckx. 2015. A swir based algorithm 787 to retrieve total suspended matter in extremely turbid waters. Remote 788 Sensing of Environment 168:66–79. https://doi.org/10.1016/j.rse.2015.06.
 - Lovelock, Catherine E. 2008. Soil respiration and belowground carbon al-791 location in mangrove forests. Ecosystems 11:342-354. ISSN: 1432-9840.792 https://doi.org/10.1007/s10021-008-9125-4.
- Lundberg, Scott M, and Su-In Lee. 2017. A unified approach to interpreting 794 738 model predictions. Advances in neural information processing systems 30.795 739 https://doi.org/10.48550/arXiv.1705.078740. 740
 - Luo, Yafei, David Doxaran, Kevin Ruddick, Fang Shen, Bernard Gentili, 797 Liwen Yan, and Haijun Huang. 2018. Saturation of water reflectance 798 in extremely turbid media based on field measurements, satellite data 799 and bio-optical modelling. Optics express 26 (8): 10435-10451. https: 800 //doi.org/10.1364/OE.26.010435.
- Marinho, Rogério Ribeiro, Tristan Harmel, Jean-Michel Martinez, and Naziano⁸⁰² Pantoja Filizola Junior. 2021. Spatiotemporal dynamics of suspended 803 747 sediments in the negro river, amazon basin, from in situ and sentinel-2 804 748 remote sensing data. ISPRS International Journal of Geo-Information 10 805 749 (2): 86. https://doi.org/10.3390/ijgi10020086. 750 806

- Markert, Kel N, Calla M Schmidt, Robert E Griffin, Africa I Flores, Ate Poortinga, David S Saah, Rebekke E Muench, Nicholas E Clinton, Farrukh Chishtie, Kritsana Kityuttachai, et al. 2018. Historical and operational monitoring of surface sediments in the lower mekong basin using landsat and google earth engine cloud computing. Remote Sensing 10 (6): 909. https://doi.org/Historicalandoperationalmonitoringofsurfacesedi mentsinthelowermekongbasinusinglandsatandgoogleearthenginecloud computing.
- Met Éireann. 2025. Historical data from current stations. https://www.met.ie/ climate/available-data/historical-data. Accessed: 2025-06-27.
- Michaels, Patrick J, Paul C Knappenberger, and Robert E Davis. 2005. Seasurface temperatures and tropical cyclones: breaking the paradigm. Presented at 15th Conference of Applied Climatology, http://ams.confex.com/ ams/15AppClimate/techprogram/paper_94127.htm.
- Mietta, Francesca, Claire Chassagne, Andrew J Manning, and Johan C Winterwerp. 2009. Influence of shear rate, organic matter content, ph and salinity on mud flocculation. Ocean Dynamics 59:751-763. https://doi. org/10.1007/s10236-009-0231-4.
- Miller, Herman C. 1999. Field measurements of longshore sediment transport during storms. Coastal engineering 36 (4): 301-321. https://doi.org/10. 1016/S0378-3839(99)00010-1.
- Montanher, Otávio Cristiano, and Edvard Elias de Souza Filho. 2015. Estimating the suspended sediment concentration in the upper paraná river using landsat 5 data: data retrieval on a large temporal scale and analysis of the effects of damming. Geografia 40 (1): 159-176.
- O'Toole, Ronan, Maria Judge, Fabio Sacchetti, Thomas Furey, Eoin Mac Craith, Kevin Sheehan, Sheila Kelly, Sean Cullen, Fergal McGrath, and Xavier Monteys. 2022. Mapping ireland's coastal, shelf and deep-water environments using illustrative case studies to highlight the impact of seabed mapping on the generation of blue knowledge. In From continental shelf to slope: mapping the oceanic realm, k. asch, h. kitazato, h. vallius, 71–96. The Geological Society of London.
- Pahlevan, Nima, John R Schott, Bryan A Franz, Giuseppe Zibordi, Brian Markham, Sean Bailey, Crystal B Schaaf, Michael Ondrusek, Steven Greb, and Christopher M Strait. 2017. Landsat 8 remote sensing reflectance (rrs) products: evaluations, intercomparisons, and enhancements. Remote sensing of environment 190:289-301. https://doi.org/10. 1016/j.rse.2016.12.030.
- Pedregosa, Fabian, Gaël Varoquaux, Alexandre Gramfort, Vincent Michel, Bertrand Thirion, Olivier Grisel, Mathieu Blondel, Peter Prettenhofer, Ron Weiss, Vincent Dubourg, et al. 2011. Scikit-learn: machine learning in python. Journal of Machine Learning Research 12:2825-2830.
- Qiu, Shi, Zhe Zhu, and Binbin He. 2019. Fmask 4.0: improved cloud and cloud shadow detection in landsats 4-8 and sentinel-2 imagery. Remote Sensing of Environment 231:111205. https://doi.org/10.1016/j.rse.2019.05.024.
- Saintilan, Neil, Katya E Kovalenko, Glenn Guntenspergen, Kerrylee Rogers, James C Lynch, Donald R Cahoon, Catherine E Lovelock, Daniel A Friess, Erica Ashe, and Ken W Krauss. 2022. Constraints on the adjustment of tidal marshes to accelerating sea level rise. Science 377 (6605): 523-527. https://doi.org/10.1126/science.abo7872.
- Shahzad, Muhammad Imran, Mohsin Meraj, Majid Nazeer, Ibrahim Zia, Asif Inam, Khalid Mehmood, and Hina Zafar. 2018. Empirical estimation of suspended solids concentration in the indus delta region using landsat-7 etm+ imagery. Journal of Environmental Management 209:254-261. https: //doi.org/10.1016/j.jenvman.2017.12.070.
- Shapley, Lloyd S, et al. 1953. A value for n-person games. Chap. 17 in Contributions to the theory of games, volume ii, 307-317. Princeton University Press Princeton. https://doi.org/10.1515/9781400881970-018.
- Suursaar, Ü, J Jaagus, and H Tõnisson. 2015. How to quantify long-term changes in coastal sea storminess? Estuarine, Coastal and Shelf Science 156:31-41. https://doi.org/10.1016/j.ecss.2014.08.001.

Syvitski, James PM, Charles J Vörösmarty, Albert J Kettner, and Pamela Green.
 2005. Impact of humans on the flux of terrestrial sediment to the global
 coastal ocean. *science* 308 (5720): 376–380. https://doi.org/10.1126/
 science.1109454.

- Tang, Yuheng, Anmin Duan, Chunyan Xiao, and Yue Xin. 2022. The prediction of the tibetan plateau thermal condition with machine learning and shapley additive explanation. *Remote Sensing* 14 (17): 4169. https://doi.org/10.3390/rs14174169.
- Vermote, Eric, Christopher O Justice, and François-Marie Bréon. 2008. To wards a generalized approach for correction of the brdf effect in modis
 directional reflectances. *IEEE Transactions on Geoscience and Remote Sensing* 47 (3): 898–908. https://doi.org/10.1109/TGRS.2008.2005977.
- Wang, Chongyang, Danni Wang, Ji Yang, Shuqing Fu, and Dan Li. 2020.
 Suspended sediment within estuaries and along coasts: a review of spatial and temporal variations based on remote sensing. *Journal of Coastal Research* 36 (6): 1323–1331. https://www.jstor.org/stable/10.2307/26952821.
- Xu, Hanqiu. 2006. Modification of normalised difference water index (ndwi)
 to enhance open water features in remotely sensed imagery. *International*journal of remote sensing 27 (14): 3025–3033. https://doi.org/10.1080/01431160600589179.
- Yepez, Santiago, Alain Laraque, Jean-Michel Martinez, Jose De Sa, Juan
 Manuel Carrera, Bartolo Castellanos, Marjorie Gallay, and Jose L Lopez.
 2018. Retrieval of suspended sediment concentrations using landsat-8
 oli satellite images in the orinoco river (venezuela). Comptes Rendus
 Geoscience 350 (1-2): 20–30. https://doi.org/10.1016/j.crte.2017.08.004.
- Zhu, Jun-Jie, Meiqi Yang, and Zhiyong Jason Ren. 2023. Machine learning in environmental research: common pitfalls and best practices. *Environmental Science & Technology* 57 (46): 17671–17689. https://doi.org/10.1021/acs.est.3c00026.